Ther Adv Respir Dis
2021, Vol. 15: 1–13
DOI: 10.1177/1753466621998246

PINK1/*Parkin*-mediated mitophagy in mechanical ventilation-induced diaphragmatic dysfunction

Hui Yong, Yun Zhou, Wanlin Ye, Tianmei Li, Gangming Wu, Jingyuan Chen, Li Liu and Jicheng Wei

Abstract

Background: Mechanical ventilation (MV) often leads to ventilation-induced diaphragm dysfunction (VIDD). Although the development of this disorder had been linked to oxidative stress, mitochondrial energy deficiency, autophagy activation, and apoptosis in the diaphragm, it remains unclear whether the activation of mitophagy can induce VIDD. With our research, our endeavor is to uncover whether PTEN-induced putative kinase 1 (PINK1)/*Parkin*-mediated mitophagy affects the MV-caused diaphragmatic dysfunction

Methods: Sprague-Dawley rats were subjected to MV treatment for 6 h (MV-6h), 12 h (MV-12h), or 24 h (MV-24h). Post MV, the diaphragm muscle compound action potential (CMAP) and cross-sectional areas (CSAs) of the diaphragm of these rats were measured. The levels of proteins of interest were examined to assess muscle health, mitochondrial dynamics, and mitophagy in the diaphragm. The co-localization of PINK1 with the mitochondrial protein marker tom20 was examined, as well as transmission electron microscopy analysis to detect changes in diaphragm mitochondrial ultrastructure.

Results: MV-12h and MV-24h treatments resulted in a decrease in CSA of diaphragm and CMAP amplitude. In addition, the expressions of F-box (MFAbx), muscle-specific ring finger 1 (MURF1), PINK1, and p62 were elevated in rats treated with MV for 12 h and 24 h, while mfn2 expression was reduced. Rats following MV-24h treatment displayed an increase in mitochondrial dynamic protein (Drp1) and *Parkin* expression and microtubule-associated protein 1 light chain 3/1 (LC3II/I) ratio. Moreover, decreased SOD and GSH activity and membrane potential were observed after MV-12h and MV-24h treatment, while H_2O_2 activity increased after MV-24h treatment. In addition, a strong co-localization between PINK1 and tom20 was identified.

Conclusion: These results reveal that MV leads to various changes in mitochondrial dynamics and significantly increases the mitophagy levels, which subsequently cause the variation in diaphragmatic function and muscle atrophy, indicating that mitophagy could be one of the possible mechanisms by which MV induces diaphragmatic dysfunction.

The reviews of this paper are available via the supplemental material section.

Keywords: diaphragmatic dysfunction, mechanical ventilation, mitochondrial autophagy

Received: 18 December 2020; revised manuscript accepted: 27 January 2021.

Correspondence to:
Li Liu
Department of Anesthesiology, The First Affiliated Hospital of Southwest Medical University, No. 25, Taiping Street, Luzhou 646000, Sichuan Province, P. R. China
niuniudoctor@swmu.edu.cn

Hui Yong
Yun Zhou
Wanlin Ye
Tianmei Li
Jicheng Wei
Department of Anesthesiology, The First Affiliated Hospital of Southwest Medical University, Luzhou, P. R. China

Gangming Wu
Jingyuan Chen
The First Affiliated Hospital of Chongqing Medical University, Chongqing, P. R. China

Introduction

The diaphragm is a thin skeletal muscle which separates the abdomen and the chest and plays a fundamental role in inhalation, contracting to draw air into the lungs. It is therefore essential that it remains rhythmically active, meaning that when this is disrupted, or if the diaphragm is unable to relax, patients must be immediately placed on mechanical ventilation (MV), a life-saving intervention. However, prolonged MV can result in rapid changes

in diaphragmatic atrophy, leading to contractile dysfunctions known as ventilation-induced diaphragm dysfunction (VIDD).[1,2] VIDD can not only have a significant poor effect on patient survival rate and prognosis, but also produces a large medical burden.[3] Under these serious life-threatening conditions, VIDD is one cause for weaning failure, becoming a challenge for health sciences.

Autophagy is a major cellular process in which damaged organelles, misfolded or aggregated proteins or pathogens are encapsulated in a double-membrane structure known as autophagosome and then degraded.[4] Mitophagy, the specific autophagic elimination of mitochondria, regulates the number of mitochondria in a cell, matching mitochondrial activity with metabolic demand as well as removing damaged mitochondria.[5] It has been reported previously that two Parkinson's disease genes, mitochondrial kinase PINK1 and ubiquitin ligase *Parkin*, can mediate damaged mitochondria degradation. Further research examining the mechanism by which these genes function revealed that the activated *Parkin* gene, a E3 ubiquitin ligase, ubiquitinylates numerous components of damaged mitochondria, directing them to lysosomes where they are degraded.[6]

A high metabolic demand means that skeletal muscles are densely packed with mitochondria. Therefore, when damaged, mitochondria in muscles produce large amounts of reactive oxygen species (ROS) which are thought to play an important role in muscle function. Recently various animal and clinical studies have shown that mitochondrial oxidative stress (MOS) is a key upstream inducer of the catabolic processes which result in muscle protein degradation. MOS also appears to be a central factor in VIDD.[1] Moreover, dysfunctional mitochondria trigger catabolic signaling pathways that can further promote the activation of muscle atrophy.[7] Interestingly, mitochondrial morphological abnormalities, such as excessive fission-fragmentation, occur immediately when patients are put on MV, meaning it is likely that mitophagy is activated.[8] Despite this, the role mitophagy plays in VIDD has not been examined. Therefore, this study set out to test the hypothesis that MV affects the activity of the PINK1/*Parkin* pathway and subsequently alters the level of mitophagy in the diaphragm, ultimately causing an imbalance in diaphragmatic protein homeostasis and causing diaphragm atrophy.

Methods

Ethics statement

All animal experiments were conducted in strict accordance with the Guide to the Management and Use of Laboratory Animals issued by the National Institutes of Health. The protocol of animal experiments was approved by the Institutional Animal Care and Use Committee of the First Affiliated Hospital of Southwest Medical University (No.: 201912-4).

Animals

Twenty-four Sprague-Dawley (SD) male rats (200–250 g) were obtained from CHENGDU DOSSY EXPERIMENTAL ANIMALS CO.LTD and used for this study. All rats were fed in a temperature-controlled (22 ± 2°C) room with a 12:12-h light–dark cycle. Rats had free access to water and food. SD rats were randomly assigned into four groups, including control group (rats served as blank control), MV-6h group (MV for 6 h), MV-12h group (MV for 12 h), and MV-24h group (MV for 24 h).

MV treatment

Rats were anesthetized by 5% pentobarbital sodium 50 mg/kg intraperitoneal injection and were fixed. Then the skin was opened by making a 2 cm surgical incision in the middle of the neck. After being bluntly separated by needle holder and vascular clamp, the rat trachea was found. Next, the 0.3 cm incision was cut transversely with ophthalmic scissors and the rat-specific endotracheal tube was inserted 1 cm by fixing with a 4.0 surgical line. The tube was then attached to a small animal special ventilator (Servoventilator 300; Siemens): tidal volume was set at 10 ml/kg, while respiratory rate was set at 80/min with an expiration ratio of 1:2.[9] Next, the vein in the right neck was separated directly and the distal vein of the heart was ligated. Then a horizontal incision (0.2 cm) was made in vascular by ophthalmic scissor. Back pumping blood by infusion pump (ZNB-XA, Vedeng, Kellymed, China) was an indication of the successful setup of the tube and whole apparatus. Anesthesia was maintained throughout by continuous pumping of sodium pentobarbital 10 mg/kg while specimens were kept on a thermostatic pad to maintain body temperature at 37.5 ± 0.5°C. Continuous care was provided during the MV procedure including the cleaning of airway mucus and eye

lubrication. When the MV time reached the required time, the rats were euthanized and the diaphragms were harvested.

The rats in the control group were maintained without access to food for 24 h before euthanasia to match their nutritional intake to the MV group.[10] Then, the rats were subjected to intraperitoneal injection of pentobarbital sodium (60 mg/kg body weight) for an acute plane of surgical anesthesia. Once a surgical plane of anesthesia was attained, the diaphragm muscle of rats was removed, and the costal diaphragm was used for mitochondria isolation.

In addition, rats after different treatment were euthanized by cervical dislocation after anesthesia with pentobarbital sodium. Hind-limb skeletal muscles (i.e. soleus, plantaris, white gastrocnemius, and red gastrocnemius) were excised, and all these hind-limb muscles were combined and used for mitochondria isolation.[11]

Muscle fiber cross-sectional areas

Segments of each diaphragm were fixed in 10% paraformaldehyde and continuous paraffin sections of approximately 8 μm thickness were taken and stained using a hematoxylin-eosin staining technique. Morphometric examination of the fibers was employed under an optical microscope (Leitz Laborhama S., Wetzlar, Germany). Then, the ross-sectional areas (CSAs) were measured and corrected for the shortening occurring from optimal length to excised length by dividing CSAs with a correction factor. This correction factor was the ratio of optimal length to unstretched length and was 1.53 for diaphragm.[12]

Non-invasive compound muscle action potential detection

The compound muscle action potential (CMAP) was detected as described previously.[13] The diaphragm muscle CMAP was recorded using the RM6240 system. The first acupuncture needle was inserted into the proximal tail subcutaneous as a ground electrode; the next acupuncture needle was inserted into the contralateral abdomen as a reference electrode; the electrode sheet was attached to the lower edge of the ipsilateral rib as a recording electrode; the last two acupuncture needles as stimulating electrodes were vertically inserted above the same side of the clavicle, 0.5 cm beside the trachea. Electrodes were inserted at a depth of 1 cm, and the distance between the two acupuncture needles was 0.5 cm. The near-heart end was connected with a red stimulation connector and the telecentric end was connected with a black stimulation connector; the stimulation mode used a single stimulus, and the mode was with positive voltage stimulation. The amplitude of the stimulus was set between 4.0 and 6.0 V, wave width at 1 ms, with a delay of 1 ms. There was 30 s interval between stimulations, and we repeated three stimulations in a row to obtain the average response.

Measurement of oxidative stress levels

Diaphragm tissues from six rats of each group were collected and placed into a pre-cooling RIPA lysis buffer (Beyotime Biotechnology, Shanghai, China). The samples were homogenized and centrifuged at 3000 rpm/minute for 15 min. Supernatant was collected and superoxide dismutase (SOD), H_2O_2 and glutathione peroxidase (GPx) were detected using an oxidative stress kit (A001; Nanjing Jiancheng Bioengineering Institute, Nanjing, China) as per the manufacturer's instructions.

Measurement of mitochondrial membrane potential.

Cytoplasmic proteins, mitochondrial proteins and high-purity mitochondria were extracted using a tissue mitochondrial isolation kit, with the whole procedure performed on ice. The mitochondrial membrane potential was measured using a JC-1 fluorescent probe. The principle for this procedure was as follows. When the mitochondrial membrane potential was high, JC-1 aggregated in the mitochondrial matrix to form a polymer that results in the production of red fluorescence. When the mitochondrial membrane potential was low, JC-1 acts as a monomer that produces green fluorescence. The JC-1 aggregate fluorescence, indicative of a high mitochondrial membrane potential, and JC-1 monomers fluorescence were detected by a microplate reader at 525 nm and 490 nm, respectively. The mitochondrial membrane potential level was expressed as the ratio of the JC-1 aggregates/JC-1 monomers.

Mitochondrial ultrastructure observation of skeletal muscle

The diaphragm was soaked in glutaraldehyde fixative. Samples were rinsed with 0.1 mol/l phosphate

buffer and fixed in 1% osmium tetroxide. After dehydration by acetone treatment, ultrathin sections of approximately 50 nm were prepared. Sections were then stained with uranyl acetate and subsequently with lead citrate at room temperature for 15–20 min. Finally, the distribution, morphology, size, structure of the mitochondria and formation of autophagosomes were observed under a JEM-1400 PLUS transmission electron microscope (TEM).

Western blot assay

The expression levels of autophagy-related proteins LC3, PINK1, *Parkin*, mitochondrial kinetics and atrophic-related proteins were detected by Western blot. The protein loading buffer was added to each sample which was then boiled for 10 min, centrifuged at 4°C for 10 min and stored. After protein separation by sodium dodecyl sulphate polyacrylamide gel electrophoresis, the proteins were transferred onto a polyvinylidene fluoride membrane at a constant voltage of 80 V. After blocking for 1 h at room temperature, the membrane was incubated overnight at 4°C with primary antibodies: mouse anti-LC3 antibody (1:1500, ab48394, Abcam, Cambridge, UK), mouse anti-pink1 antibody (1:1500, Cat#6946, Cell Signaling Technology, Beverly, Massachusetts, USA), and mouse anti-parkin antibody (1:1500, Cat#4211, Cell Signaling Technology, Beverly, Massachusetts, USA). Finally, after overnight incubation, the membrane was further incubated with secondary antibody for 1 h at room temperature, and developed by ECL.

Immunofluorescence

Paraformaldehyde-fixed samples were dehydrated with sucrose, embedded, and sliced. Sections were then immersed in 0.01 M citrate buffer (pH 6.0), rinsed with PBS, and 10% serum blocking solution was added dropwise at room temperature for 30 min. Primary antibodies were added at 4°C overnight, while the secondary antibodies were added to the sample at 37°C for 30 min. DAPI was added at room temperature for 10 min. After that, the anti-fluorescence attenuating capsule was used for sealing. Images were collected by section using a fluorescence microscope camera system. Each section was observed at 100× before the whole tissue and then three fields were selected to acquire 400×.

Statistical analysis

SPSS 17.0 and Image-Pro plus software were used for statistical analysis. Quantitative test results were expressed as means ± SEM throughout this study. One-way analysis of variance was used for comparison between groups. $p < 0.05$ was considered statistically significant (two-tailed).

Results

Neuromuscular electrophysiology

The amplitude of CMAP: There was no significant difference between the control group (6.41 ± 1.32 mv) and the MV-6h group (4.67 ± 0.46 mv) ($p > 0.05$). Compared with the control group, the CMAP amplitude statistically decreased in the MV-12h group (3.15 ± 0.52 mv) and MV-24 group (2.44 ± 1.26 mv) ($p < 0.05$) (Figure 1a).

The time course of CMAP: There was no significant difference in between the control group (2.8 ± 0.15 ms), the MV-6h group (3.07 ± 0.32 ms), and the MV-12h group (3.48 ± 0.43 ms) ($p > 0.05$). The difference between the control group and the MV-24 group (7.05 ± 0.61 ms) was statistically significant ($p < 0.05$) (Figure 1b).

Diaphragm fiber CSAs

Compared with the control group (5308.67 ± 228.18 um^2), the diaphragm fiber CSAs of the MV-6h (3378.33 ± 393.40 um^2), MV-12h (2969.67 ± 35.16 um^2), and MV-24h (2115.33 ± 130.23 um^2) groups were reduced. These differences were statistically significant ($p < 0.05$) (Figure 2).

Variation in muscular atrophy-related proteins expression

Compared with the control group, MFAbx and MURF1 in the MV-12h group and the MV-24h group were significantly increased ($p < 0.05$) (Figure 3).

MV inhibits SOD and GSH activity and increases the H_2O_2 level

Compared with the control group, SOD activity in the MV-12h group and the MV-24h group were significantly decreased ($p < 0.05$). GSH

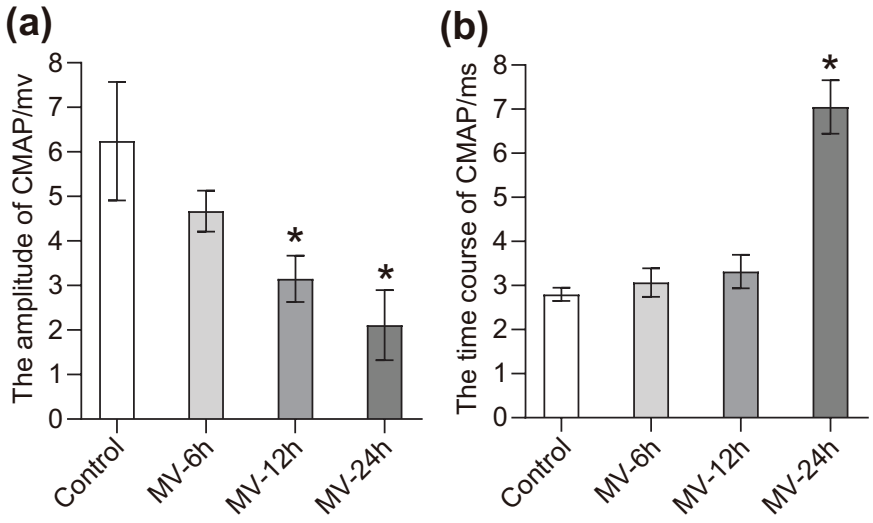

Figure 1. CMAP analysis of the diaphragm. (a) The amplitude of CMAP of each group; and (b) The time course of CMAP of each group.
The measurement data were expressed as mean ± standard deviation. The experiment was performed at least three times. Data among multiple groups were analyzed by one-way ANOVA, with Tukey's *post hoc* test.
*$p < 0.05$ compared with blank group.

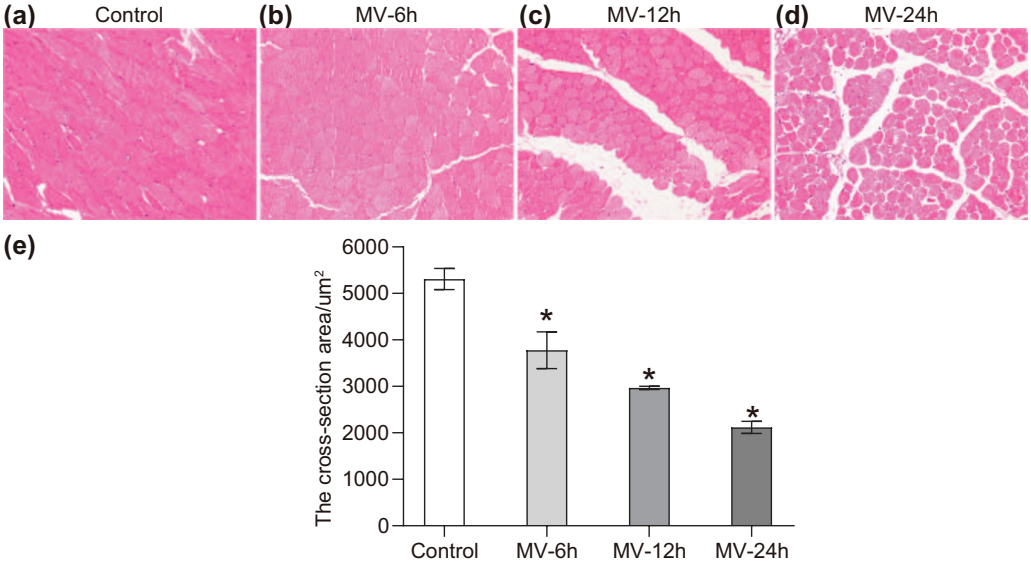

Figure 2. The CSAs of diaphragm muscle fibers in each group. (a) Representative image of the control group; (b) Representative image of the MV-6h group; (c) Representative image of the MV-12h group; (d) Representative image of the MV-24h group; and (e) The statistical results of the CSAs in each group.
The measurement data were expressed as mean ± standard deviation. The experiment was performed at least three times. Data among multiple groups were analyzed by one-way ANOVA, with Tukey's *post hoc* test.
*$p < 0.05$ compared with blank group.

activity in the MV-6h group, the MV-12h group and the MV-24h group were also significantly decreased ($p < 0.05$), and H_2O_2 activity in the MV-24h group was notably increased ($p < 0.05$) (Figure 4).

The changes of mitochondrial membrane potential

When the mitochondrial membrane potential was lowered, the JC-1 aggregate decreased while the monomer ratio was increased. It resulted in a

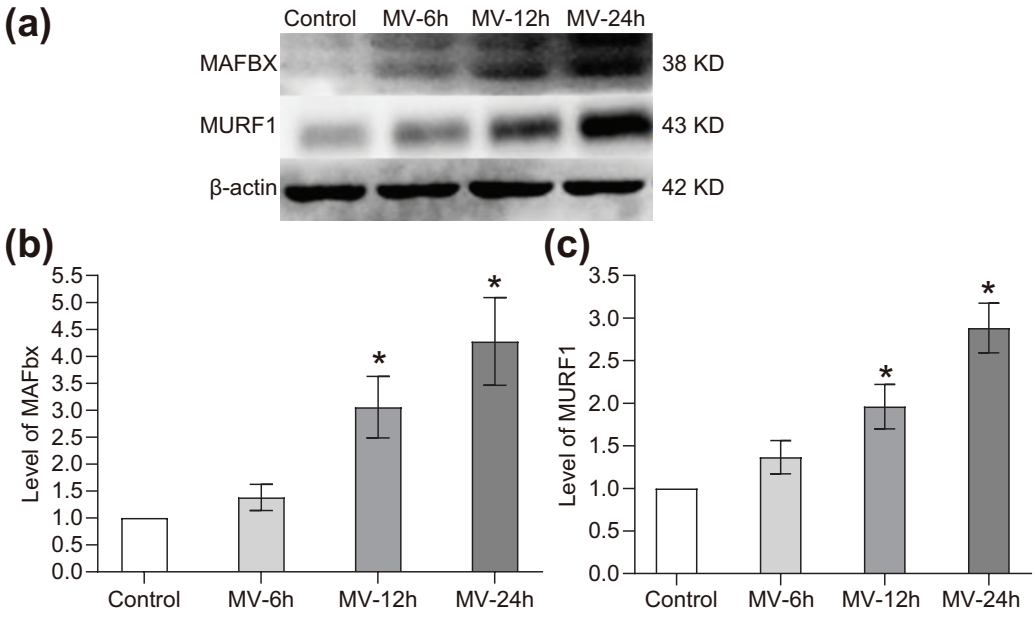

Figure 3. Protein expression of MFABX and MURF1 in each group. (a) Protein bands of MFABX and MURF1 by Western blot; (b) Protein expression of MFABX in each group; and (c) Protein expression of MURF1 in each group.
The measurement data were expressed as mean ± standard deviation. The experiment was performed at least three times. Data among multiple groups were analyzed by one-way ANOVA, with Tukey's *post hoc* test.
*$p < 0.05$ compared with blank group.

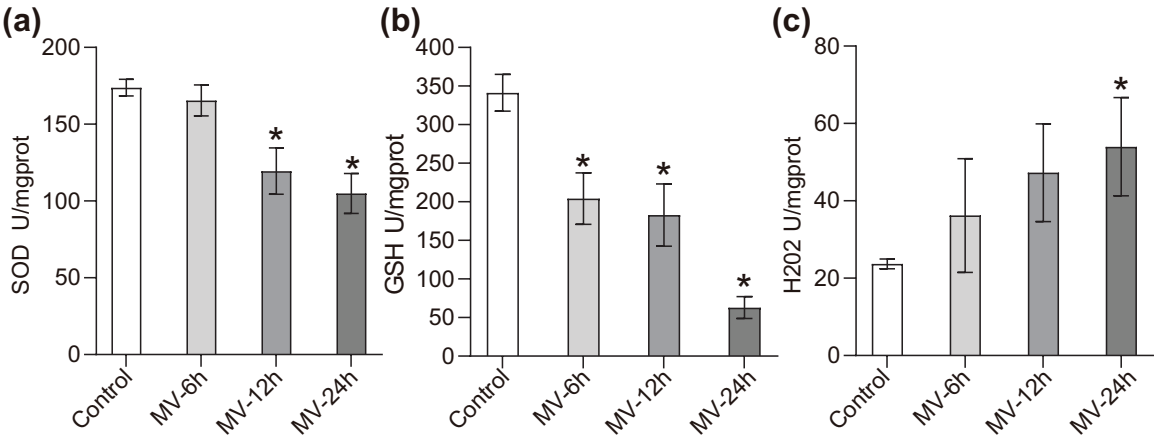

Figure 4. Production of SOD, GSH, and H_2O_2 in each group. (a) SOD content; (b) GSH content; and (c) H_2O_2 content.
The measurement data were expressed as mean ± standard deviation. The experiment was performed at least three times. Data among multiple groups were analyzed by one-way ANOVA, with Tukey's *post hoc* test.
*$p < 0.05$ compared with blank group.

decrease of red fluorescence and an increase of green fluorescence, and the ratio of the membrane potential was reflected by the red/green fluorescence ratio. Compared with the control group, the aggregates of the MV-12h group and the MV-24h group were significantly decreased ($p < 0.05$) (Figure 5).

The changes in mitochondrial ultrastructure of skeletal muscle

TEM imaging revealed that mitochondria were swollen and fragmented with disorganized cristae, and also exhibited decreased matrix density. In the control group, the mitochondrial structures

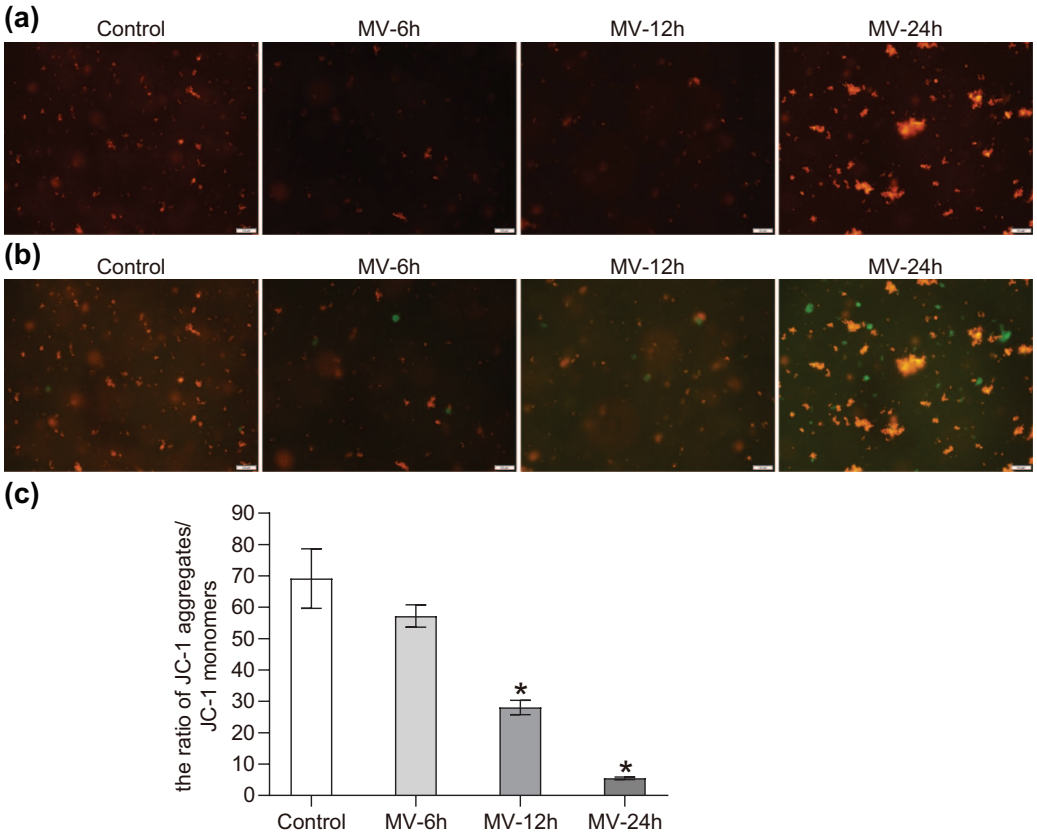

Figure 5. Comparison of the mitochondria membrane potential of each group (*$p < 0.05$). (a) The red fluorescence of each group; (b) The green fluorescence of each group; and (c) The membrane potential of each group; the ratio was calculated by red/green fluorescence ratio.
The measurement data were expressed as mean ± standard deviation. The experiment was performed at least three times. Data among multiple groups were analyzed by one-way ANOVA, with Tukey's *post hoc* test.
*$p < 0.05$ compared with blank group.

were generally intact (Figure 6a). In the MV-6h group, the mitochondria began to swell, and cristae disappeared (Figure 6b). In the MV-12h group, the swelling of the mitochondria was evident. Moreover, at this time point, a small number of autophagosomes and mitophagy also begin to appear between myofibrils (Figure 6c). In the MV-24 group, in addition to autophagosomes and mitophagy, a large number of lipid droplets were also identified (Figure 6d). Overall, the diaphragm of the rats in the control group remained normal, while the degree of mitochondrial swelling or cristae disappeared with the prolongation of MV.

The change of proteins of mitophagy in the diaphragm

Compared with the control group, Drp1 increased significantly in MV24h and mfn2 decreased in the MV-12h and MV-24h groups ($p < 0.05$) (Figure 7a); compared with the control group, PINK1 increased significantly in the MV-12h group and the MV-24h group, *Parkin* increased in the MV-24h group while P62 was increased in the MV-12h group and MV-24h group ($p < 0.05$). The LC3II/I ratio was increased in the MV-24h group ($p < 0.05$) (Figure 7b).

Gradual increase in autophagosomes and mitophagy was observed with the prolongation of MV

To further determine the occurrence of mitophagy, the co-localization of Pink1 protein with the mitochondrial protein marker tom20 was determined using confocal microscopy. Initially, the autophagosomes were rarely seen in the control group; however, with the prolongation of MV the numbers of autophagosomes were significantly increased in MV-24h group ($p < 0.05$) (Figure 8a and b).

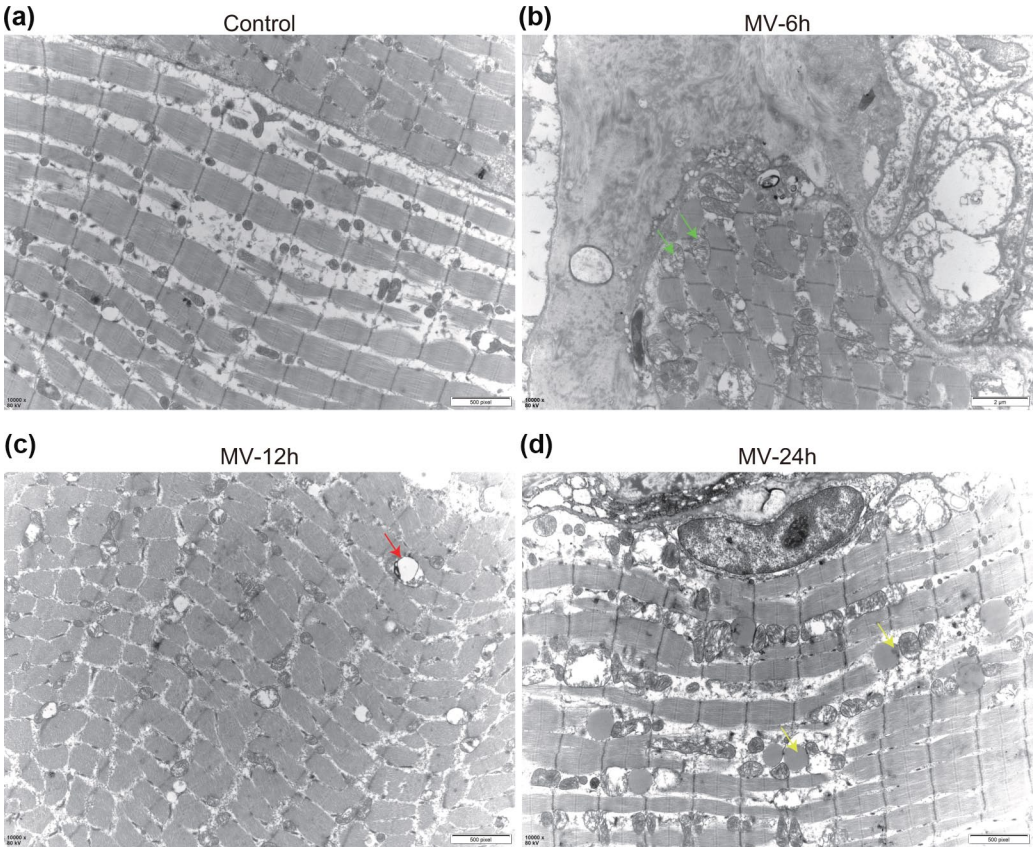

Figure 6. Morphologic abnormalities of mitochondria and autophagy in the diaphragm. (a) Representative TEM results in the control group showed normal ultrastructure and the absence of autophagosomes; (b) Representative TEM images from the MV-6h group, showing mitochondria are swollen and fragmented, with disorganized cristae (green arrows); (c) Representative TEM images from the eMV-12h group, showing autophagosomes and swollen mitochondria (green arrows); and (d) Representative TEM images from the MV-24h group, showing lipid droplets (yellow arrows).
M, mitochondria; N, nucleus.

Surprisingly, we observed the co-localization of PINK1 and tom20, with lots of overlapping areas being observed in the MV-24h (Figure 8d).

Discussion

Numerous cellular processes have previously been linked to the development of VIDD, including oxidative stress, mitochondrial energy deficiency, activation of autophagy and apoptosis.[8] However, prior to this study, whether the activation of mitophagy can induce VIDD has not been examined. The present study uncovers the relationship between mitophagy and VIDD. Our experimental data support the hypothesis that MV can cause significant changes in diaphragmatic function and histology, increased mitochondrial fission and reduced fusion, as well as an increased level of mitophagy. We demonstrate that there is a strong relationship between mitophagy and VIDD.

Numerous studies have shown that prolonged MV leads to VIDD.[14,15] However, the precise mechanism by which MV induces VIDD remains unclear and is of significant therapeutic significance. Here we address this experimental question using an artificial ventilation rat model where rats are secured to a ventilator for a range of different time periods, after which muscle atrophy can be examined. Interestingly, atrophy-related proteins MAFbx and MURF1 were shown to significantly increase in expression as ventilation times were increased from 12 h to 24 h. In contrast, the CSA of the MV-6h group was significantly lower than in the MV-12h group and MV-24h groups.

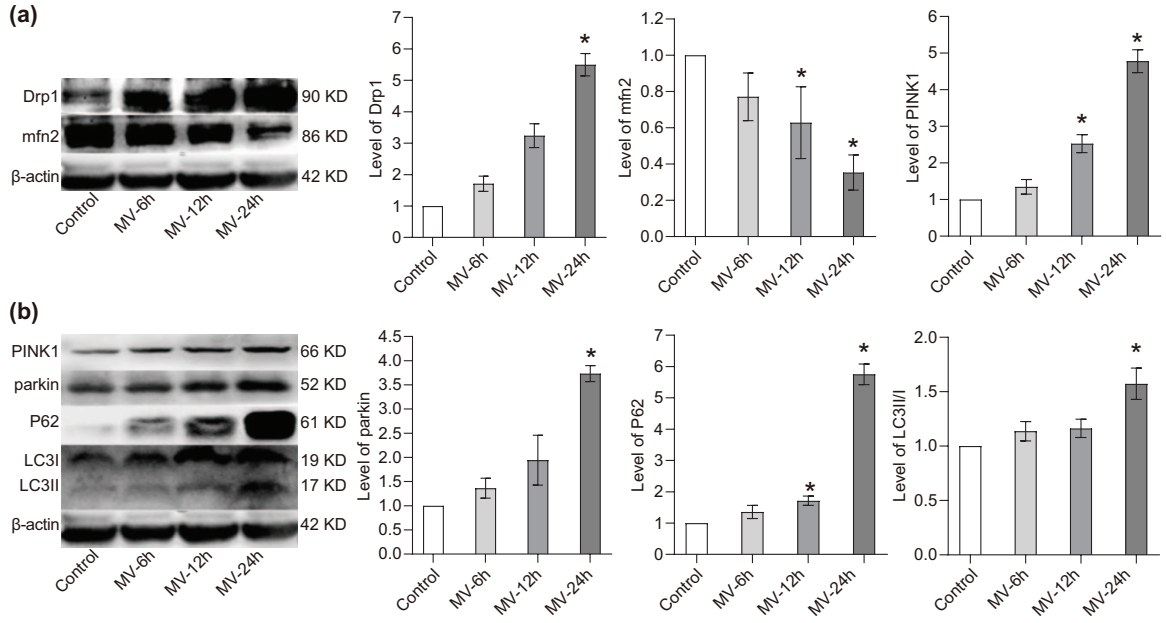

Figure 7. The level of protein of mitophagy in each group (*$p < 0.05$). (a) The protein expression of Drp1, Mfn2, and PINK1 in each group. The Western blot protein bands are shown in the left panel and the corresponding quantitative results are shown in the right panel; and (b) the protein expression of PINK1, *Parkin*, P62 and LC3II/I in each group. The Western blot protein bands are shown in the left panel and the corresponding quantitative results are shown in the right panel.
The measurement data are expressed as mean ± standard deviation. The experiment was performed at least three times. Data among multiple groups were analyzed by one-way ANOVA, with Tukey's *post hoc* test.
*$p < 0.05$ compared with blank group.

With only four major time points being studied in this project, and with patients often spending a prolonged period on MV, future work should focus on VIDD occurrence following longer ventilation periods.

Currently, it is generally believed that MOS is the primary factor which induces VIDD.[1] Concurrently, it was first reported in 2002 that prolonged MV could trigger oxidative stress and lead to diaphragmatic damage in rats.[16] MV could trigger abnormal mitochondrial dynamics and morphology in the diaphragm, which has also been demonstrated previously.[8] A large number of subsequent studies examining both human and animal models have confirmed the association between VIDD and increased oxidative stress in the diaphragm. It is well known that mitochondria are the main source of ROS production in the diaphragm.[17,18] Accordingly, Smuder *et al.*[19] suggested that enhanced autophagy and ROS form a feedback loop which is activated by oxidative stress, leading to runaway production of ROS and subsequent rates of autophagy. Moreover, earlier reports have shown that in response to ROS, mitochondrial membrane potential ($\Delta\Psi m$) significantly decreases, ultimately resulting in the translocation of *Parkin* to the damaged mitochondria.[20] Consistent with these findings, our experimental data demonstrate that the ROS level was significantly increased in MV-12h and MV-24h, emphasizing the fact that oxidative stress is inseparably linked to VIDD and potentially responsible for provoking the VIDD mechanism. In line with our results, it has been uncovered that prevention of MV-induced increases in diaphragmatic mitochondrial ROS emission protects against MV-induced diaphragmatic weakness.[18] This important finding further validates mitochondria as a primary source of ROS production in the diaphragm during prolonged MV, which indicates the important involvement of VIDD in mitochondrial diseases, especially the ROS imbalance.

Mitochondria are dynamic organelles that continually pass through fusion and fission events while also interacting with adjacent organelles to reshape their structure and function, a process which is collectively known as mitochondrial dynamics.[8] Drp1 is thought to be an essential protein during

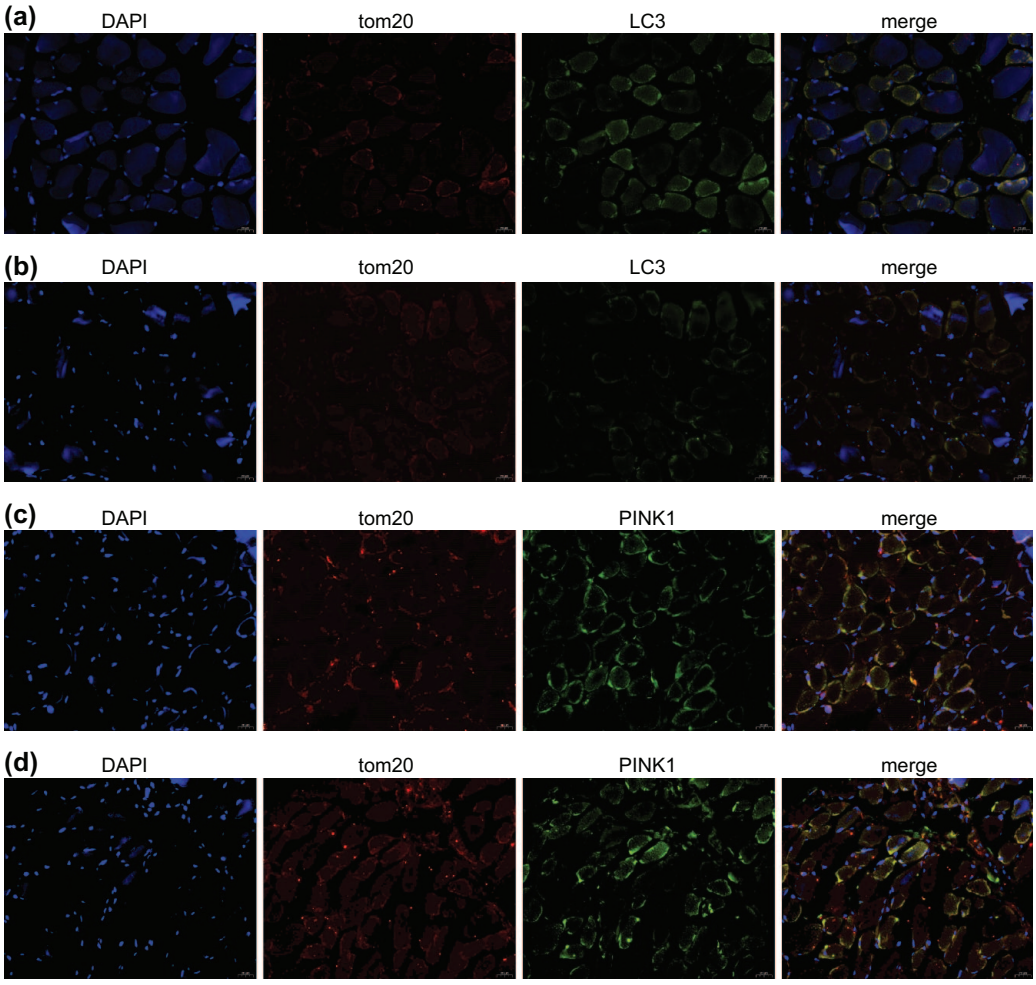

Figure 8. The co-localization of LC3 and PINK1 with tom20, respectively. (a) In the control group, autophagosomes were rarely observed; (b) the MV-24h group showed a comparatively high amount of green LC3 fluorescence mention autophagosome; (c) the control group has a small amount of overlapping areas that represent the co-localization of PINK1 and mitochondria; and (d) there were lots of co-located areas of PINK1 and tom20 in the MV-24h group.

mitochondrial fission. However, rat knockout studies have provided clear evidence that MFN is critical for mitochondrial fusion.[21] Moreover, Romanello *et al.*[22] have demonstrated that by triggering organelle dysfunction and AMPK activation, expression of the mitochondrial fusion machinery is increased and that these changes are sufficient to induce muscle atrophy in adult animals. This disruption of the mitochondrial network is considered to be an amplified cycle which is mainly responsible for muscular atrophy. On the other hand, mfn2 is essential for the maintenance of stable mitochondria, stabilizing both mitochondrial DNA and its membranes. Downregulation of mfn2 could enhance mitochondrial division and subsequently drive fragmentation, further accelerating the mitochondrial autophagic degradation.[23]

Building on these findings, the present study demonstrates that, in comparison to the control group, the mitochondrial fission protein Drp1 expression levels gradually increased while the fusion protein mfn2 decreased in MV treated group. However, it is worth noting that the 24 h period with a lack of food supply may slightly affect these results. These findings may indicate that MV can cause significant changes in mitochondrial dynamics. With increased time periods spent on MV, rates of mitochondrial fission increased, with a decrease in the fusion being observed, which may accelerate mitochondrial autophagy and lead to the occurrence of VIDD.

The PINK1/*Parkin* pathway has been considered an important pathway in the regulation of mitophagy.[24] In healthy mitochondria, PINK1 is degraded by the PARL protein after entering the mitochondria through the outer membrane translocating enzymes and the endometrial transposase complex. Therefore, PINK1 remains at a lower level in the cytoplasm.[25] Generally, *Parkin* is an E3 ligase that is self-suppressing; when inactive it is held in a closed state by a variety of intramolecular interactions. When mitochondria are damaged or depolarized, PINK1 is activated and aggregates on the mitochondrial outer membrane. PINK1 has ability to directly phosphorylate *Parkin* and can also activate *Parkin* indirectly through phosphorylated ubiquitin.[26] Activated *Parkin* can accumulate a large number of ubiquitin chains that further attach to numerous substrates located on the mitochondria outer membrane, resulting in protein ubiquitination on the membrane.[27] The ubiquitinated mitochondria are then recognized by the adaptor protein P62 and an autophagic receptor protein (with a region interacting with LC3) linked to LC3 on the autophagic vesicle membrane. Finally, upon the formation of mitochondrial autophagosomes, mitophagy is induced.[28] Our study showed that the mitochondrial membrane potential significantly decrease in the MV-12h and MV-24h. Furthermore, by measuring the levels of proteins that are essential for mitophagy, such as PINK1, *Parkin*, P62, LC3, we found that mitophagy is activated by MV time, while a clear linear relationship between mitophagy and time spent of MV was evident. Our results from TEM analysis confirmed the presence of mitophagy and that, with increased ventilation time, the degree of mitochondrial swelling and the disappearance of the cristae increased. Finally, results from immunofluorescence experiments show that with prolonged MV, autophagosomes and co-localization of PINK1 and tom20 increased. It is therefore clear that MV induced mitophagy in the diaphragm.

It has been well established that when the energy supply far exceeds the cellular requirements, it can trigger an increase in mitochondrial ROS.[29] For instance, in rats, hyperlipidemia can aggravate diaphragmatic oxidative stress during MV, with an excess of energy being an important factor in this process.[17] The main reason for this abnormality could be due to diaphragm inactivity during MV. Decreased contractile activity of the diaphragm during MV alters the energy balance in the muscle, which could further decrease mitochondrial biogenesis and enzymatic activity and may lead to increased lipid accumulation and oxidative stress.[17] Additionally, in the case of excess energy metabolism and increased intramuscular lipids, lipids in muscle cells can react with ROS and become a potential source of oxidative stress,[30] thereby accelerating the cycle of free radical generation and mitochondrial dysfunction.[31] Interestingly, TEM analysis post MV demonstrated that there were lots of lipid droplets following prolonged MV. It is therefore possible that prolonged MV leads to an excess of energy stores in the diaphragm which underpin the observed mitochondrial instability.

Conclusion

In summary, our results indicate that VIDD may cause prolonged periods of MV and that this correlates with clear increase in mitochondria autophagy. It is therefore possible that mitophagy may be a critical signaling pathway in the formation of VIDD. This provides insight into VIDD formation which could have therapeutic implications both with VIDD prevention and treatment, as well as potential drug targets.

Acknowledgements

We give our sincere gratitude to the reviewers for their valuable suggestions.

Conflict of interest statement

The authors declare that there is no conflict of interest.

Funding

The authors disclosed receipt of the following financial support for the research, authorship, and/or publication of this article: This study was supported by the National Natural Science Foundation of China (No. 81772128).

ORCID iD

Li Liu https://orcid.org/0000-0002-3090-6562

Supplemental material

The reviews of this paper are available via the supplemental material section.

References

1. Tang H and Shrager JB. The signaling network resulting in ventilator-induced diaphragm dysfunction. *Am J Respir Cell Mol Biol* 2018; 59: 417–427.
2. Vassilakopoulos T and Petrof BJ. Ventilator-induced diaphragmatic dysfunction. *Am J Respir Crit Care Med* 2004; 169: 336–341.
3. Bruells CS, Marx G and Rossaint R. [Ventilator-induced diaphragm dysfunction: clinically relevant problem]. *Anaesthesist* 2014; 63: 47–53.
4. Yang HW, Menon LG, Black PM, *et al.* SNAI2/Slug promotes growth and invasion in human gliomas. *BMC Cancer* 2010; 10: 301.
5. Youle RJ and Narendra DP. Mechanisms of mitophagy. *Nat Rev Mol Cell Biol* 2011; 12: 9–14.
6. Bingol B and Sheng M. Mechanisms of mitophagy: PINK1, Parkin, USP30 and beyond. *Free Radic Biol Med* 2016; 100: 210–222.
7. Zhang YY, Gu LJ, Huang J, *et al.* CKD autophagy activation and skeletal muscle atrophy-a preliminary study of mitophagy and inflammation. *Eur J Clin Nutr* 2019; 73: 950–960.
8. Picard M, Azuelos I, Jung B, *et al.* Mechanical ventilation triggers abnormal mitochondrial dynamics and morphology in the diaphragm. *J Appl Physiol (1985)* 2015; 118: 1161–1171.
9. Lellouche F, Dionne S, Simard S, *et al.* High tidal volumes in mechanically ventilated patients increase organ dysfunction after cardiac surgery. *Anesthesiology* 2012; 116: 1072–1082.
10. Azuelos I, Jung B, Picard M, *et al.* Relationship between autophagy and ventilator-induced diaphragmatic dysfunction. *Anesthesiology* 2015; 122: 1349–1361.
11. Kavazis AN, Talbert EE, Smuder AJ, *et al.* Mechanical ventilation induces diaphragmatic mitochondrial dysfunction and increased oxidant production. *Free Radic Biol Med* 2009; 46: 842–850.
12. Stassijns G, Gayan-Ramirez G, De Leyn P, *et al.* Systolic ventricular dysfunction causes selective diaphragm atrophy in rats. *Am J Respir Crit Care Med* 1998; 158: 1963–1967.
13. Martin M, Li K, Wright MC, *et al.* Functional and morphological assessment of diaphragm innervation by phrenic motor neurons. *J Vis Exp* 2015: e52605.
14. Hudson MB, Smuder AJ, Nelson WB, *et al.* Both high level pressure support ventilation and controlled mechanical ventilation induce diaphragm dysfunction and atrophy. *Crit Care Med* 2012; 40: 1254–1260.
15. Tang H, Lee M, Khuong A, *et al.* Diaphragm muscle atrophy in the mouse after long-term mechanical ventilation. *Muscle Nerve* 2013; 48: 272–278.
16. Shanely RA, Zergeroglu MA, Lennon SL, *et al.* Mechanical ventilation-induced diaphragmatic atrophy is associated with oxidative injury and increased proteolytic activity. *Am J Respir Crit Care Med* 2002; 166: 1369–1374.
17. Picard M, Jung B, Liang F, *et al.* Mitochondrial dysfunction and lipid accumulation in the human diaphragm during mechanical ventilation. *Am J Respir Crit Care Med* 2012; 186: 1140–1149.
18. Powers SK, Hudson MB, Nelson WB, *et al.* Mitochondria-targeted antioxidants protect against mechanical ventilation-induced diaphragm weakness. *Crit Care Med* 2011; 39: 1749–1759.
19. Smuder AJ, Sollanek KJ, Nelson WB, *et al.* Crosstalk between autophagy and oxidative stress regulates proteolysis in the diaphragm during mechanical ventilation. *Free Radic Biol Med* 2018; 115: 179–190.
20. Narendra D, Tanaka A, Suen DF, *et al.* Parkin is recruited selectively to impaired mitochondria and promotes their autophagy. *J Cell Biol* 2008; 183: 795–803.
21. Lee H and Yoon Y. Mitochondrial fission and fusion. *Biochem Soc Trans* 2016; 44: 1725–1735.
22. Romanello V, Guadagnin E, Gomes L, *et al.* Mitochondrial fission and remodelling contributes to muscle atrophy. *EMBO J* 2010; 29: 1774–1785.
23. Zhao J, Brault JJ, Schild A, *et al.* FoxO3 coordinately activates protein degradation by the autophagic/lysosomal and proteasomal pathways in atrophying muscle cells. *Cell Metab* 2007; 6: 472–483.
24. Yin J, Guo J, Zhang Q, *et al.* Doxorubicin-induced mitophagy and mitochondrial damage is associated with dysregulation of the PINK1/Parkin pathway. *Toxicol In Vitro* 2018; 51: 1–10.
25. Lazarou M, Jin SM, Kane LA, *et al.* Role of PINK1 binding to the TOM complex and alternate intracellular membranes in recruitment and activation of the E3 ligase Parkin. *Dev Cell* 2012; 22: 320–333.

26. Kondapalli C, Kazlauskaite A, Zhang N, *et al.* PINK1 is activated by mitochondrial membrane potential depolarization and stimulates Parkin E3 ligase activity by phosphorylating Serine 65. *Open Biol* 2012; 2: 120080.

27. Mouton-Liger F, Jacoupy M, Corvol JC, *et al.* PINK1/Parkin-dependent mitochondrial surveillance: from pleiotropy to *Parkin*son's disease. *Front Mol Neurosci* 2017; 10: 120.

28. Lan R, Wu J-T, Wu T, *et al.* Mitophagy is activated in brain damage induced by cerebral ischemia and reperfusion via the PINK1/Parkin/p62 signalling pathway. *Brain Res Bull* 2018; 142: 63–77.

29. Lecuona E, Sassoon CS and Barreiro E. Lipid overload: trigger or consequence of mitochondrial oxidative stress in ventilator-induced diaphragmatic dysfunction? *Am J Respir Crit Care Med* 2012; 186: 1074–1076.

30. Schrauwen P, Schrauwen-Hinderling V, Hoeks J, *et al.* Mitochondrial dysfunction and lipotoxicity. *Biochim Biophys Acta* 2010; 1801: 266–271.

31. Bugger H and Abel ED. Molecular mechanisms for myocardial mitochondrial dysfunction in the metabolic syndrome. *Clin Sci (Lond)* 2008; 114: 195–210.